

# Resonant spin-changing collisions in spinor Fermi gases

N. Bornemann, P. Hyllus and L. Santos

*Institut für Theoretische Physik, Leibniz Universität Hannover, Appelstr. 2, D-30167, Hannover, Germany*

Spin-changing collisions in trapped Fermi gases may acquire a resonant character due to the compensation of quadratic Zeeman effect and trap energy. These resonances are absent in spinor condensates and pseudo-spin-1/2 Fermi gases, being a characteristic feature of high-spin Fermi gases that allows spinor physics at large magnetic fields. We analyze these resonances in detail for the case of lattice spinor fermions, showing that they permit to selectively target a spin-changing channel while suppressing all others. These resonances allow for the controlled creation of non-trivial quantum superpositions of many-particle states with entangled spin and trap degrees of freedom, which remarkably are magnetic-field insensitive. Finally, we show that the intersite tunneling may lead to a quantum phase transition described by an effective quantum Ising model.

Cold spinor gases have recently attracted a large interest. A spinor gas is formed by atoms in two or more internal states simultaneously confined by optical traps [1]. Particularly intense efforts have been devoted to spinor Bose-Einstein condensates (BECs), which present a rich variety of ground state phases with different topologies [2, 3, 4, 5, 6], such as ferromagnetic, polar, uni- and bi-axial nematic, and more. Spinor Fermi gases are also attracting currently a growing attention. Collective modes in high-spin fermions have been shown to present rich features [7]. Spin-1 Fermions allow for color superfluidity and baryon formation, linking spinor fermion physics to QCD [8]. Spin-3/2 fermions also present fascinating properties such as quintet Cooper pairing and Alice strings [9].

The dynamics of spinor BECs has been also actively investigated, in particular the coherent oscillations between spinor components [10]. In addition, spinor gases constitute a novel tool for the analysis of out-of-equilibrium systems, and the generation of topological defects after a rapid quenching across a phase transition [11]. On the contrary the spinor dynamics of high-spin fermions has been, to the best of our knowledge, not studied in detail.

An external magnetic field typically constitutes a major handicap for the spinor dynamics. Although, due to spin conservation during a collision, the linear Zeeman effect (LZE) is irrelevant for the spinor dynamics, the quadratic Zeeman effect (QZE) may become (even for relatively low fields) sufficient to suppress spin change collisions, and hence any spinor dynamics [10]. However, under appropriate conditions an external magnetic field may even stimulate spin dynamics in spinor BECs, due to the compensation of QZE and mean-field shifts [12].

In the following, we show that spinor fermions allow for controllable magnetically-tuned resonances in the spin-changing dynamics, by compensating QZE and trap energy. These resonances are typically absent in spinor BECs, either because the mean-field energy greatly overwhelms the trap energy in the Thomas-Fermi regime, or because in the weakly-interacting regime the trap levels are irrelevant since the bosons mainly occupy the ground state of the trap. In lattice arrangements, as those dis-

cussed below, low temperature bosons occupy the lowest energy band, and hence the resonances play no role. They are also absent in pseudo-spin-1/2 fermions, since due to spin conservation the QZE energy is conserved. On the contrary, these resonances constitute a characteristic feature of high-spin trapped Fermi gases.

In this Letter we illustrate the role of these resonances for the case of fermions with spin  $f = (2s+1)/2$  ( $s \geq 1$ ) in an optical lattice, where each site acts as an independent anharmonic trap, with up to three relevant levels (filling factor per spin component  $\bar{n} < 3$ ). However, we stress that the compensation between QZE and trap energy should also play an important role in more general optical traps, leading to trap-dependent resonant spinor dynamics, which will be the subject of a forthcoming work. Here, we study these resonances in detail for the lattice case, including interaction-induced shifts and resonance splittings, analyzing how for  $f \geq 5/2$  these resonances may be employed to select particular spin-changing collisions while suppressing all others. Additionally, we show that an adiabatic sweep through the resonances allows for the controlled creation of quantum superpositions of states with entangled spin and trap degrees of freedom. These states are magnetic-field insensitive, and hence, contrary to the usual case, these systems allow for the study of spinor physics at large magnetic fields. Finally, we discuss the effect of the inter-site tunneling, showing that under proper conditions it may be described by a quantum Ising Hamiltonian, hence leading to a quantum phase transition between different multiparticle states as a function of the tunneling rate.

The independent sites are described by the Hamiltonian  $\hat{H} = \hat{H}_0 + \hat{H}_B + \hat{H}_I$ . The trap energy is given by

$$H_0 = \sum_{n=0}^2 E(n) \sum_{m=-f}^f \hat{a}_{n,m}^\dagger \hat{a}_{n,m}, \quad (1)$$

where  $E(n) = \hbar\omega(n + \beta n^2)$ , and  $\hat{a}_{n,m}$  is the annihilation operator of fermions of spin  $m$  in the trap level  $n$ . The effective trap frequency ( $\omega$ ) and anharmonicity ( $\beta$ ) are obtained from the calculated first three on-site energies. The state of the system is described by a Fock state of

the form:  $|N_{0,-f}, \dots, N_{2,f}\rangle \equiv \prod_{n=0}^2 \prod_{m=-f}^f (a_{n,m}^\dagger)^{N_{n,m}}$ , where we keep the order (from left to right) from  $(n = 0, m = -f)$  to  $(n = 2, m = f)$  [13].

The effects of a magnetic field  $B$  are given by

$$\hat{H}_B = \sum_{n,m} (-pm + qm^2) \hat{a}_{n,m}^\dagger \hat{a}_{n,m}, \quad (2)$$

where the LZE is given by  $p = g\mu_B B$ , with  $g$  the Landé factor and  $\mu_B$  the Bohr magneton, and the QZE by  $q = \mu_B^2 B^2 / 4\hbar\omega_{hs}$ , where  $\omega_{hs}$  is the hyperfine splitting.

Finally, the interatomic interactions (which we consider as being dominantly of short-range character) are provided by a Hamiltonian of the form [2]

$$\hat{H}_I = \frac{1}{2} \sum_{\vec{n}, \vec{m}} C_{\vec{n}} U_{\vec{m}} \hat{a}_{n_4, m_4}^\dagger \hat{a}_{n_3, m_3}^\dagger \hat{a}_{n_2, m_2} \hat{a}_{n_1, m_1}, \quad (3)$$

where  $\vec{n} = \{n_1, n_2, n_3, n_4\}$ ,  $\vec{m} = \{m_1, m_2, m_3, m_4\}$ ,  $C_{\vec{n}} = \int d^3r \phi_{n_4}(\vec{r})^* \phi_{n_3}(\vec{r})^* \phi_{n_2}(\vec{r}) \phi_{n_1}(\vec{r})$ , and  $U_{\vec{m}} = \sum_{F,M} g_F \langle f, m_1, m_2 | FM \rangle \langle FM | f, m_3, m_4 \rangle$ . In these expressions,  $g_F = 4\pi\hbar^2 a_F / m$ , with  $a_F$  the scattering length for the collisional channel with total spin  $F$  (which due to symmetry must be an even number),  $M = -F, \dots, F$ ,  $\langle f, m_1, m_2 | FM \rangle$  are the Clebsch-Gordan coefficients, and  $\phi_n(\vec{r})$  the  $n$ -th trap eigenfunction. The dynamics is calculated by integrating the corresponding many-body Schrödinger equation, using Runge-Kutta techniques.

Although the resonances discussed below should be observable for general initial conditions, the analysis of the effects implied is simplified by considering an initial mixture of  $m = \pm 1/2$  (at the end of this Letter we discuss how this mixture may be achieved in on-going experiments). In addition, this initial state may be employed, as shown below, to controllably create complex superpositions of spin-level entangled states. For a filling factor (per component)  $\bar{n} = n_0 + \delta n$ , with  $n_0 = 0, 1, \dots$ , all levels up to  $n_0 - 1$  are filled in all sites, whereas the level  $n_0$  is occupied with a probability  $\delta n$ . This imprecise filling becomes eventually important, and is taken into account in our simulations. For  $\bar{n} = 2$ , state  $|1\rangle$  in Fig. 1 is the initial state for the dynamics.

A collision leads to a QZE shift  $\Delta E_{QZE} = q(m_3^2 + m_4^2 - m_1^2 - m_2^2)$ . As discussed above, this shift prevents spin-change collisions, as long as  $|\Delta E_{QZE}|$  is larger than the typical interaction energy of spin-change collisions. Level-changing collisions are characterized by an energy shift  $\Delta E_{TRAP} = E(n_4) + E(n_3) - E(n_2) - E(n_1)$ . An interesting situation occurs when spin-changing collisions are at the same time level-changing. In that case,  $\Delta E_{QZE}$  and  $\Delta E_{TRAP}$  may compensate each other, leading to resonances in the spin-changing collisions. Spin conservation precludes these resonances in usual spin-1/2 Fermi systems, which thus do not show level-changing collisions if  $|\Delta E_{TRAP}|$  is larger than the spin-changing interaction energy. In the following, and for simplicity of our discussion, we concentrate in situations where

the harmonic trap energy can be assumed as conserved ( $n_1 + n_2 = n_3 + n_4$ ), and only the anharmonic change  $\Delta E_{ANH} = \beta\hbar\omega(n_3^2 + n_4^2 - n_1^2 - n_2^2)$  is relevant. In general, however, a sufficiently large  $B$  may lead to resonances which involve a violation of the previous condition, leading to a wealth of resonances and complex multiparticle superpositions, similar to those discussed below.

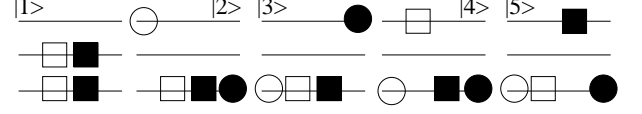


Figure 1: States involved in the resonant dynamics at  $\alpha \simeq -1/2$  for  $f = 3/2$ . The lines indicate from bottom to top the three trap levels. The spin states are indicated by filled and hollow squares ( $m = \pm 1/2$ ) and circles ( $m = \pm 3/2$ ).

The resonances are altered by interparticle interactions. We illustrate this by considering the initial  $f = 3/2$  state  $|1\rangle$  (see Fig.1). Note that multi-particle states  $|2\rangle$  to  $|5\rangle$  possess equal QZE plus anharmonic energy,  $E_{QZE} + E_{ANH} = 5q + 4\beta\hbar\omega$  (an important point as discussed below), whereas for  $|1\rangle$   $E_{QZE} + E_{ANH} = q + 2\beta\hbar\omega$ . Hence a resonance would be expected at  $\alpha \equiv \frac{q}{\beta\hbar\omega} = -1/2$ . However, a detailed analysis shows that close to resonance the states indicated in Fig. 1 are isolated from the rest of all other possible (seven) states that can be reached via  $\hat{H}_I$  from  $|1\rangle$ , leading to an effective 5-state problem. Interestingly, one may show that  $|D_1\rangle \equiv (|3\rangle + |2\rangle)/\sqrt{2}$ , and  $|D_2\rangle \equiv (|5\rangle + |4\rangle)/\sqrt{2}$  decouple from  $|1\rangle$ , playing a similar role as dark-states in quantum optics. The dynamics is then fully dominated by the coupling of  $|1\rangle$  and two “bright” states  $|\pm\rangle = \frac{1}{2}[(|3\rangle - |2\rangle) \pm (|5\rangle - |4\rangle)]$ . As a consequence, the resonance splits into two peaks, corresponding to the energy shifts between  $|1\rangle$  and  $|\pm\rangle$ :

$$\alpha_R = -1/2 + [g_0\xi_0 + g_2(\xi_1 \pm \delta\xi)] / 4\beta\hbar\omega \quad (4)$$

where  $\xi_0 = C_{1100} - C_{2200} + C_{1111}/2$ ,  $\xi_1 = -2C_{0000} - 3C_{2200} + C_{1100} + C_{1111}/2$ , and  $\delta\xi = 2C_{2200}$ . Note that, due to the EPR-like nature of the spin-change collisions, the resonances are accompanied by transitions into quantum superpositions of multi-particle states with entangled spin and trap level degrees of freedom, which we explore below. Split resonances for  $1 < \bar{n} < 2$  (Fig. 2) are hence a direct consequence of the coherent formation of the above mentioned many-body entangled states. The split resonance peak may be employed to selectively detect  $|\pm\rangle$  (which may become important to probe the linear superpositions discussed below), since initial  $|+\rangle$  or  $|-\rangle$  states lead to different shifts of the resonance into  $|1\rangle$ , observable by monitoring the  $m = 1/2$  population. The picture gets more complicated if  $2 < \bar{n} < 3$  (Fig. 2), since the resonances are shifted depending whether there is none, one or two particles in the third trap level. Multiple resonance peaks appear (or a resonance broadening

if the individual peaks are not resolved), but in this case due to the imprecise filling, as well as to the above mentioned splitting. Since the spinor dynamics depends on  $\bar{n}$ , one observes plateaux in  $d^2 N_{3/2}/d\bar{n}^2$  (where  $N_{3/2}$  is the sum of the time-averaged populations in  $m = \pm 3/2$ ), with jumps when  $\bar{n}$  becomes an integer (resembling the de Haas-van Alphen susceptibility plateaux).

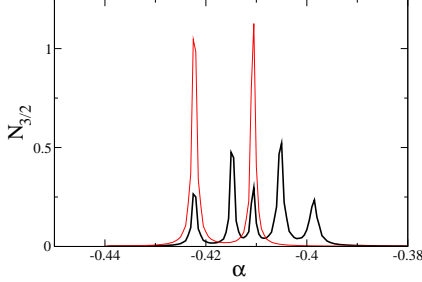


Figure 2: (color online)  $f = 3/2$ . Time-averaged population ( $N_{3/2}$ ) in  $m = \pm 3/2$  as a function of  $\alpha$ , for  $\tilde{g}_{0,2} = 0.08, 0.10$  [14], and  $\bar{n} = 2.0$  (thin, red), and  $2.5$  (thick).

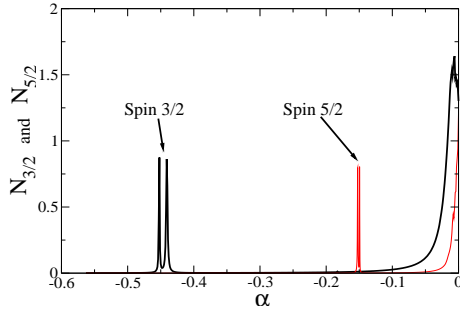


Figure 3: (color online)  $f = 5/2$ . Time averaged population  $N_{3/2}$  in  $m = \pm 3/2$  (thick) and  $N_{5/2}$  in  $m = \pm 5/2$  (thin, red) as a function of  $\alpha$ , for  $\bar{n} = 2.0$ , and  $\tilde{g}_{0,2,4} = 0.08, 0.10, 0.05$  [14].

Whereas for  $f = 3/2$  only one spin-changing collisional channel is possible,  $f \geq 5/2$  allows for more channels. Fig. 3 shows the case of spin-5/2. Note that with an initial state  $|1\rangle$  only two spin-changing collisions are possible: from  $(n_{1,2} = 1; m_{1,2} = \pm 1/2)$  either into  $(n_{3,4} = 0, 2; m_{3,4} = \pm 3/2)$  or  $(n_{3,4} = 0, 2; m_{3,4} = \pm 5/2)$ , with respective resonances at  $\alpha_R \simeq -1/2$  and  $\alpha_R \simeq -1/6$ . Interestingly, if the two resonances are well resolved, as it is the case in Fig. 3, it may be possible to select a particular spin-changing channel, preventing all others, providing a novel tool for the manipulation of spinor gases. As for the  $f = 3/2$ , the resonances couple the initial states with non trivial superpositions of spin-level entangled states.

As previously mentioned, quantum superpositions of spin-level entangled states play an important role in the dynamics at the spin-changing resonances. These states may be created in a controllable way by sweeping adiabatically the external magnetic field across the resonances. As an example, we consider the spin-3/2 case. If

$\beta < 0$ , the state  $|1\rangle$  is the ground-state for  $|\alpha| > |\alpha_R|$ . In that case, if  $g_2 > 0$  ( $g_2 < 0$ ) an adiabatic sweep towards  $|\alpha| < |\alpha_R|$  creates  $|+\rangle$  ( $|-\rangle$ ), with a fidelity larger than 95% for sweeps with  $d\alpha/dt = 2.5 \times 10^{-4} \frac{\omega}{2\pi}$ . If the gas is prepared initially at  $\alpha = \alpha_R - 0.05$ , this linear ramp towards  $\alpha = \alpha_R + 0.05$  demands a change in 4000 trap periods, which for typical values of the effective on-site  $\omega$  (few  $kHz$ ) represents sweep times of less than 0.5s. Note that for  $\beta < 0$ , the created states are the ground-states for  $|\alpha| < |\alpha_R|$ , except for  $g_2 < 0, g_0 > -3g_2$  and  $g_2 > 0, g_0 > g_2$ , where  $D_{1,2}$  are the (degenerate) ground states. However, as mentioned above, these states are dark states and hence they are not coupled to  $|1\rangle$  during the sweep. Note that remarkably, all states belonging to the superpositions  $|\pm\rangle$  possess the same QZE. This leads to two important consequences. On one hand, the sweep across the resonance is produced at rather large  $B$  ( $\sim 1$  G, see below), but the result of the sweep crucially depends on the spinor physics (sign of  $g_2$ ). Hence spinor physics becomes relevant even for large  $B$ . Second, once the states are produced an abrupt increase of  $B$  leaves the system unchanged, and hence the superpositions created may be robust at very large  $B$ , even opening the possibility of employing Feshbach resonances to variate  $g_2$  or  $g_0$ , without polarizing the system due to the QZE. Similar states may be created by adiabatic sweeps for  $f > 3/2$ . E.g., for  $f = 5/2$  a sweep would create a state  $\cos(\phi)(|2\rangle - |3\rangle)/\sqrt{2} + \sin(\phi)(|4\rangle - |5\rangle)/\sqrt{2}$ , where  $\tan \phi = (\epsilon - \sqrt{\epsilon^2 + \Omega^2})/\Omega$ ,  $\epsilon = 15(2g_2 - g_4)(C_{0220} - C_{0000})/42$ , and  $\Omega = 2(9g_4 - 2g_2 - 7g_0)C_{1102}/7$ .

The states discussed above are created in isolated lattice sites. However, if the lattice is relaxed, the tunneling for the third band may become relevant, especially if the splitting  $4g_2 C_{0220}$  between the states  $|\pm\rangle$  becomes very small. In that case, different types of lattice Hamiltonians may be created. Let us consider the particular case of spin-3/2, with  $|g_2| \ll |g_0|$ . In that case, the states  $|\pm\rangle$  form a quasidegenerate pseudo-spin-1/2 doublet. If the tunneling  $t$  for the third band satisfies  $t \ll |g_0|$ , then second order processes lead to an effective spin Hamiltonian. Note that the condition  $|g_2| \ll |g_0|$  is necessary to avoid mixing other possible states. Employing  $|+\rangle\langle+| = 1/2 + \hat{S}^z$ ,  $|-\rangle\langle-| = 1/2 - \hat{S}^z$ ,  $|+\rangle\langle-| = \hat{S}^x + i\hat{S}^y$ ,  $|-\rangle\langle+| = \hat{S}^x - i\hat{S}^y$ , the effective lattice Hamiltonian may be reduced to a quantum Ising Hamiltonian [16]

$$\hat{H}_{eff} = -J_{eff} \sum_i \hat{S}_i^z - W_{eff} \sum_{\langle i,j \rangle} \hat{S}_i^x \hat{S}_j^x \quad (5)$$

where  $J_{eff} = 4g_2 C_{0220}$ , and  $W_{eff} = \frac{4t^2}{3g_0 C_{0220}} \frac{2C_{2222} - 3C_{0220}}{C_{2222} - 3C_{0220}}$ . Typically  $W_{eff} > 0$  ( $< 0$ ) if  $g_0 > 0$  ( $< 0$ ). Hence there is a critical tunneling,  $t_c^2 = 3g_2 g_0 C_{0220}^2 \left( \frac{C_{2222} - 3C_{0220}}{2C_{2222} - 3C_{0220}} \right)$ , such that for  $t < t_c$  the single-site physics dominates, and  $|+\rangle$  ( $|-\rangle$ ) is the ground-state for  $g_2 > 0$  ( $g_2 < 0$ ). For  $t > t_c$  the tunneling dominates, and for  $g_0 > 0$  the system

enters into a ferromagnetic state with all sites in either  $|u\rangle \equiv (|3\rangle - |2\rangle)/\sqrt{2}$  or  $|d\rangle \equiv (|5\rangle - |4\rangle)/\sqrt{2}$ . If  $g_0 < 0$  the coupling is antiferromagnetic, and hence a 1D system enters into a staggered configuration with alternated  $|u\rangle$  and  $|d\rangle$  states. The latter case opens the possibility for the analysis of frustration in other lattice geometries.

Finally, we comment on possible experimental realizations. We stress that the resonances should play an important role in high-spin Fermi gases in general dipole traps. For the case discussed above, the resonances should be clearly observable in standard lattices,  $V_0 \sin^2 \kappa x$ . However, these lattices may be inappropriate for the detailed study of the rich phenomena discussed, since very large  $V_0 > 50E_{rec}$  (where  $E_{rec} = \hbar^2 \kappa^2 / 2m$ ) is needed to isolate the three lowest levels at each site from other sites, and it may be difficult to load only the first three bands of an initially weak lattice, due to the vanishing gap  $\Delta E_{34}$  between the third and fourth band. A better scenario is provided by trimerized lattices (three wells per elementary cell) [15]. In our calculations we have considered for simplicity a 1D trimerized lattice  $V(x) = V_0(\sin^2(\kappa x/3) + \frac{1}{2}\cos^2(2\kappa x/3) + \frac{3}{4}\sin^2(\kappa x))$ , assuming a strong confinement in the  $yz$ -plane provided e.g. by an additional 2D lattice.  $V(x)$  allows for a relatively large  $\Delta E_{34}$  even for relatively weak lattices. E.g. for  $V_0 = 0.5E_{rec}$ ,  $\Delta E_{34} \simeq 0.22E_{rec}$  (for, e.g.,  $^{40}\text{K}$ , typically  $E_{rec}/k_B \simeq 2\mu\text{K}$ ), whereas the tunneling for the lowest bands is still sufficiently large (allowing for thermalization in the weak lattice). In this way, it may be possible to prepare controllably a Fermi gas in the first three bands, if the temperature  $T < \Delta E_{34}$  and  $\bar{n} < 3$ . The considered initial  $m = \pm 1/2$  mixture may be created from a polarized Fermi gas in a maximally stretched state, by first employing an adiabatic radio-frequency sweep to transfer into  $m = 1/2$ , and then a  $\pi/2$  radio-frequency pulse to establish a coherent  $m = \pm 1/2$  mixture. A sufficiently large  $B$  (away from the discussed resonances) isolates this mixture against spin-change collisions due to QZE. In the presence of polarized bosons (e.g. in KRb mixtures), this mixture would thermalize in the weak lattice leading to an incoherent  $m = \pm 1/2$  mixture, which after a lattice ramp-up would lead to the isolated sites discussed in this Letter. In a last stage the bosons should be eliminated, and  $B$  brought to the resonant values. For  $^{40}\text{K}$ ,  $q/\hbar \simeq 70 (\frac{B}{\text{G}})^2 \text{ Hz}$ , hence for  $2\pi/\kappa = 800\text{nm}$  and  $V_0 = 3.3E_{rec}$  ( $\omega/2\pi \simeq 9.25\text{kHz}$ ,  $\beta = -0.3$ ),  $\alpha = -1/2$  occurs for  $B \simeq 4.45\text{G}$ .

Summarizing, spin-changing collisions in Fermi gases become resonant if the QZE compensates the trap energy. These resonances are absent in BECs and spin-1/2 Fermi gases, being a characteristic feature of high-spin fermions. We have shown for the case of lattice fermions that the resonances are shifted and split by interactions, and may permit to target a single spin-changing channel while avoiding the rest. The resonances allow for the controlled creation of quantum superpositions of states with

entangled spin and trap-level degrees of freedom. These superpositions are magnetically isolated, and hence these systems allow for the observation of spinor physics at large magnetic fields, in principle even at Feshbach resonances. Finally, tunneling may compete with the on-site spinor physics to lead to a quantum phase transition described by a quantum Ising model. The rich phenomenology deriving from these resonances is by no means exhausted by the discussion above. Interesting physics is expected in the spinor dynamics of high-spin fermions in dipole traps. In addition, different resonances and spin mixtures in lattice fermions may allow for a wealth of quantum superpositions of spin-level entangled states, and various types of effective Hamiltonians. These perspectives will be the focus of forthcoming works.

We thank C. Klempt, Th. Henninger, and J. Arlt for useful discussions. This work was supported by the DFG (SFB-TR21, SFB407, SPP1116).

- 
- [1] J. Stenger *et al.*, Nature **396**, 345 (1998).
  - [2] T.-L. Ho, Phys. Rev. Lett. **81**, 742 (1998).
  - [3] T. Ohmi and K. Machida, J. Phys. Soc. Jpn. **67** 1822 (1998).
  - [4] M. Koashi and M. Ueda, Phys. Rev. Lett. **84**, 1066 (2000); C. V. Ciobanu, S.-K. Yip, and T.-L. Ho, Phys. Rev. A **61**, 033607 (2000).
  - [5] R. B. Diener and T.-L. Ho, Phys. Rev. Lett. **96**, 190405 (2006); L. Santos and T. Pfau, Phys. Rev. Lett. **96**, 190404 (2006).
  - [6] H. Mäkelä, Y. Zhang and K.-A. Suominen, J. Phys. A:Math. Gen. **36**, 8555 (2003); R. Barnett, A. Turner and E. Demler, Phys. Rev. Lett. **97**, 180412 (2006).
  - [7] S. Yip and T.-L. Ho, Phys. Rev. A **59**, 4653 (1999).
  - [8] A. Rapp *et al.*, Phys. Rev. Lett. **98**, 160405 (2007).
  - [9] C. Wu, Mod. Phys. Lett. **20**, 1707 (2006).
  - [10] M. D. Barret, J. A. Sauer, and M. S. Chapman, Phys. Rev. Lett. **87**, 010404 (2001); H. Schmaljohann *et al.*, Phys. Rev. Lett. **92**, 040402 (2004); M.-S. Chang *et al.*, Phys. Rev. Lett. **92**, 140403 (2004); T. Kuwamoto *et al.*, Phys. Rev. A **69**, 063604 (2004); M. H. Wheeler *et al.*, Phys. Rev. Lett. **93**, 170402 (2004); J. M. Higbie *et al.*, Phys. Rev. Lett. **95**, 050401 (2005).
  - [11] W. H. Zurek, U. Dorner, and P. Zoller, Phys. Rev. Lett. **95**, 105701 (2005); L. E. Sadler *et al.*, Nature **443**, 312 (2006).
  - [12] J. Kronjäger *et al.*, Phys. Rev. Lett. **97**, 110404 (2006).
  - [13] When operating with  $\hat{a}_{nm}$  and  $\hat{a}_{nm}^\dagger$ , the Wigner-Jordan factors become crucial.
  - [14]  $\tilde{g}_F = g_F/2\pi l_\perp^2 l_x \hbar \omega$ , where  $l_x^2 = \hbar/m\omega$ , and  $l_\perp = \hbar/m\omega_\perp$ , where  $\omega_\perp$  denotes the transversal confinement (see discussion at the end of the Letter). E.g. for a transversal 2D lattice  $V_1(\sin(\kappa y)^2 + \sin(\kappa z)^2)$ , with  $V_1 = 10E_{rec}$ , and  $V_0 = 3.33E_{rec}$ ,  $\tilde{g}_F = 0.1$  represents  $a_F \simeq 1.65nm$ .
  - [15] L. Santos *et al.*, Phys. Rev. Lett. **93**, 030601 (2004).
  - [16] S. Sachdev, "Quantum Phase transitions", Cambridge University Press (Cambridge, 1998).